Control by the Circulation Transport Outside the Arctic on Transient Response of AMOC to Global Warming

Jiao Chen[1], Xidong Wang[1,2], Xuezhu Wang[3], and Tido Semmler[3,4]

[1] *Key Laboratory of Marine Hazards Forecasting, Ministry of Natural Resources, Hohai University, Nanjing, China*.

[2] *Southern Marine Science and Engineering Guangdong Laboratory (Zhuhai), Zhuhai, China.*

[3] *Alfred Wegener Institute, Helmholtz Centre for Polar and Marine Research, Bremerhaven, Germany*

[4] *Met Eireann, Dublin, Ireland*

Corresponding author: Xidong Wang (xidong_wang@hhu.edu.cn)

Key Points:

- Transient response of Atlantic overturning circulation to global warming is dominated by circulation adjustment due to outer-Arctic warming
- Advection heat transport and local heat fluxes dominate the weakening of deep convection in Nordic Seas and Labrador Sea, respectively
- Deep convection weakening in Nordic Seas is more pronounced than in Labrador Sea

Abstract

Using the Alfred Wegener Institute Climate Model (AWI-CM 1.1 LR), we conduct sensitivity experiments separating the Arctic and extra-Arctic warming to investigate the transient response of AMOC to quadrupled carbon dioxide (4×CO2) forcings. The results suggest that AMOC weakening is primarily affected by circulation adjustment induced by the outer-Arctic warming, while the effects of Arctic warming are confined to the polar range and contribute less to AMOC changes. When warming forcing is applied outside the Arctic, the increases of northward advective heat transport dominate the weakening of deep convection in the Nordic Seas, while the reduction of heat loss from ocean to atmosphere is prevalent in Labrador Sea. Besides, the weakening of deep convection in Nordic Seas is more pronounced than in Labrador Sea, implying a leading role of Nordic Seas in the weakening of AMOC under global warming.

Plain Language Summary

The Atlantic Meridional Overturning Circulation (AMOC) is a large-scale circulation with significant impacts on climate system, the mechanisms of which are complex and not yet fully understood. We use the Alfred Wegener Institute Climate Model (AWI-CM 1.1 LR) to separate and quantify the AMOC response to climate warming by applying quadrupled carbon dioxide (4×CO2) forcings. The results suggest that AMOC weakening mainly result from the circulation adjustment induced by warming outside the Arctic, and the effect of Arctic warming is relatively weak and limited to polar regions. The Nordic Seas and Labrador Sea are two key areas for deep convection. Difference in local variability between these two areas is due to the distinct relative contributions of advective heat transport and net surface heat fluxes. In warming conditions, the increase of northward advection heat transport into Nordic Seas is the main factor, while in Labrador Sea, the heat loss reduction from ocean to atmosphere dominates. The process of local

stratification enhancement and deep convection weakening in the Nordic Seas is much more significant than effect of heat loss reduction in the Labrador Sea, indicating that the Nordic Seas play a more important role in the weakening of AMOC under global warming.

1 Introduction

As a key indicator of global ocean circulation, Atlantic Meridional Overturning Circulation (AMOC) plays a critical role in the climate system (Liu et al., 2020; McManus et al., 2004; Zhao et al., 2018). The adjustment of such large-scale circulation has substantial implications on ocean heat exchange, carbon uptake, and global ecosystems (e.g., Li et al., 2020; Suzuki et al., 2022). However, the persistent increase in CO2 emissions may lead to irreversible climate change in the coming millennium (Solomon et al., 2009). Extensive research is currently focused on describing and understanding changes in the AMOC and its response to anthropogenic warming (e.g., Levang & Schmitt, 2020; Lique & Thomas, 2018). Despite the discrepancy in results, the prevailing observational and modeling evidence has pointed out that AMOC has weakened or will soon weaken in response to global warming (e.g., Chen & Tung, 2018; Liu et al., 2020).

Based on millennial-length simulations, Bonan et al. (2022) found that most models consistently simulate an AMOC weakening in the early centuries, but exhibit diverse recovery behaviors afterward. The ocean response to climate warming on shorter timescales is better captured by the coupled model(e.g., Haskins et al., 2020; He et al., 2019). Simulation results suggest that the warming of the North Atlantic governs centennial-scale AMOC, while longer timescale changes are related to Southern Ocean (Jansen et al., 2018; Thomas & Fedorov, 2019). Both the sea ice melting in the Arctic, and the temperature anomalies and circulation shifts outside the Arctic can cause local changes in the subpolar region(e.g., Semmler et al., 2020a; Smedsrud et

al., 2022). Similarly, understanding the AMOC response to global warming requires identifying the impacts and relative contributions of oceanic processes in different latitudes.

The AMOC delivers warm and salty waters in its upper limb into the subpolar region of the North Atlantic (Chafik et al., 2014), where they transformed into dense deep-water in the lower limb via buoyancy loss (Medhaug et al., 2012; Suzuki et al., 2022). Therefore, the production of dense water in the North Atlantic largely governs the strength of AMOC (Lozier et al., 2019). Previous views considered Nordic Seas and Labrador Sea as the two main areas of deep convection (Medhaug et al., 2012). Some studies also suggested that the overflow water in Nordic Sea is the key to AMOC state(e.g., Chafik & Rossby, 2019). Petit et al. (2020) revealed that the deep-water formation occurs primarily in the Iceland Basin and Irminger Sea by local buoyancy forcing. The key challenge is to explore the variability of deep convection in the North Atlantic and its modulation of AMOC in global warming scenarios.

Here, we are specifically interested in what happens over the following century after the sudden onset of forcing. To explore the transient response of AMOC to the increase of greenhouse gas on a century scale, this study adopts a set of sensitivity experiments with perturbation in coupled models inspired by Stuecker et al. (2018). Through sensitivity experiments, we separate and distinguish the effects of Arctic and extra-Arctic as the increasing CO2 concentration prescribed in different regions. The simulation may help better understand the adjustment of large-scale ocean circulation in response to anthropogenic warming and provide a reference for climate projection.

2 Materials and Methods

The simulation employs the Alfred Wegener Institute Climate Model version 1.1 (AWI-CM 1.1) which incorporates the atmosphere component ECHAM 6.3 and ocean component, i.e., Finite Element Sea Ice-Ocean Model FESOM 1.4 (Semmler et al., 2020a). In this study, we conduct a control (CTRL) run in which CO2 concentration is kept at 1950 level (313 ppm) and three sensitivity runs with the CO2 concentration quadrupled in different latitudes. The sensitivity experiments with 4×CO2 forcing throughout the runs north of 60°N, south of 60°N, and globally are referenced to as 60N, 60NS, and GLOB runs, respectively. The 60N and 60NS experiments are set up to decompose the oceanic response to forcing in different regions. The CTRL experiment runs for 200 years, with the initial 50 years taken as spin-up and thereafter each sensitivity experiment runs for 150 years. We chose simulation of the last 110 years to analyze the AMOC response to the regional 4×CO2 forcings. More detailed description of model and experiment setup can be found in supplementary Text S1 and Table S1.

To investigate the stability of deep convection areas, the average stratification is computed. The average stratification is defined as the regionally weighted average squared buoyancy frequency of water column within the mixed-layer depth (MLD) (Thomas & Ferrari, 2008):

$$\overline{N^2} = -\frac{1}{H}\int_H^0 \frac{g}{\rho}\frac{\partial\langle\rho\rangle}{\partial z}dz \qquad (1)$$

where g is the gravitational acceleration, H is the regionally averaged MLD which is defined in terms of density with a fixed threshold of 0.03 kg m^{-3}, ρ is the potential density, and '$\langle\ \rangle$' denotes the laterally weighted average of the deep convection region. According to the deepest convection of modern record (1987-1994) at Labrador Sea since 1983 (Yashayaev, 2007;

Yashayaev & Loder, 2017), we define the March MLD exceeding 2500 m in the subpolar north Atlantic as the main deep convection zone (see Supplementary Figure S1). We chose March to represent the late winter months when maximum deep convection occurs in high latitudes of Northern Hemisphere (Levang & Schmitt, 2020).

Based on the linearized state equation with time-depth-varying coefficients (Fofonoff & Millard, 1983; McDougall, 1987), we decompose the total stratification of the ocean into thermal and saline parts for a better assessment of the relative contribution of temperature and salinity to the stratification changes:

$$\overline{N_t^2} = \frac{1}{H}\int_H^0 g\alpha \frac{\partial \langle T \rangle}{\partial z} dz \quad (2)$$

$$\overline{N_s^2} = -\frac{1}{H}\int_H^0 g\beta \frac{\partial \langle S \rangle}{\partial z}\, dz \quad (3)$$

where α and β are the thermal expansion and haline contraction coefficient of water, T and S are the potential temperature and salinity. $\overline{N_t^2}$ and $\overline{N_s^2}$ represent the contribution term of temperature and salinity, respectively ($\overline{N^2} \approx \overline{N_t^2} + \overline{N_s^2}$).

3 Results

3.1 AMOC Response to Warming Forcing

Semmler et al. (2020a) quantified the influence of regional greenhouse gas forcing on the atmosphere climate and point out that warming outside the Arctic has a stronger impact on Arctic and mid-latitudes than warming in the Arctic. We examine the AMOC strength in ocean when regional quadrupled CO2 forcing is applied to the first century. All sensitivity experiments exhibit a shoaling of AMOC depth, defined as the lower boundary of the upper overturning cell where stream function nearly equals zero (see the grey bold line in Figure 1). However, the depth

of maximum value of AMOC remains almost unchanged in response to 4×CO2 forcings prescribed in different latitudes. The AMOC strength is defined as the maximum value of zonally and depth-integrated transport along 45 °N in Atlantic Ocean. The climatological means AMOC strength in CTRL is 16.5±1.1 Sv. Compared to CTRL run, the climatological AMOC strength in GLOB run decreases by 4.9 Sv, which is nearly equivalent to the sum of the reduction in 60N (1.5 Sv) and 60 NS (3Sv).

Even though ocean response to global warming is not linear, the similarity of the superposition results suggests that the experimental setup is reasonable. Notably, the AMOC response to extra-Arctic warming differs somewhat from the one to Arctic warming. In 60N, AMOC strength decreases slightly, while in 60NS it weakens significantly and is more similar to the AMOC variation in GLOB than that in 60N (Figure 1). The degree of AMOC weakening is highly dependent on the location where the CO2 forcing is prescribed, and the results of different sensitivity experiments imply that warming outside Arctic can account for more than 65% of the AMOC response. The initial AMOC weakening on centennial time scales is generally attributed to variations over North Atlantic (Bonan et al., 2022; Suzuki et al., 2022). March-mean MLD variability in deep convection zone has been established to be a good indicator of convective mixing and deep-water formation (Thomas et al., 2015). The late winter convection in CTRL run exceeds 2500 m at the central Nordic Seas and Labrador Sea. When the CO2 forcing is prescribed in Arctic (60N), deep convection slightly weakens and is close to CTRL. In contrast, the March MLD reduces dramatically and even no more than 1000 m in 60NS and GLOB (Supplementary Figure S1), indicating a general weakening and shoaling of AMOC in the global warming scenario.

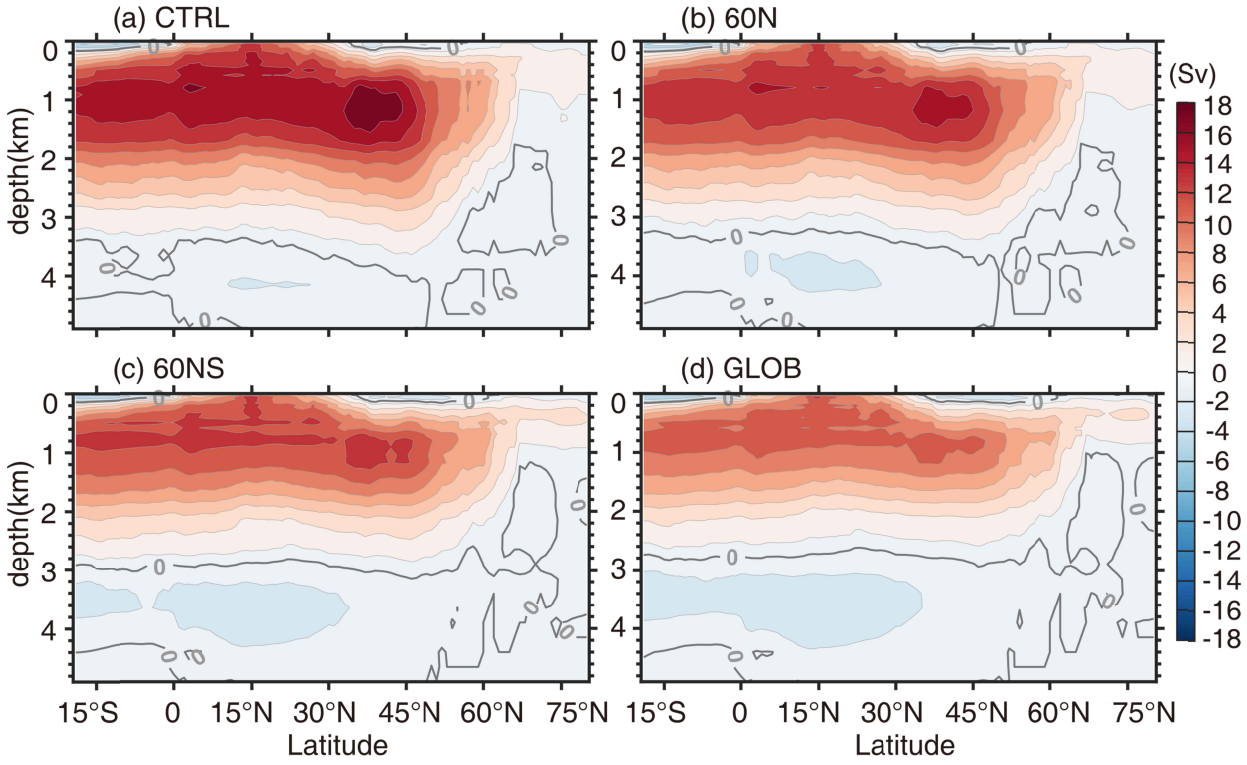

Figure 1. Climatology AMOC stream function (Sv) between 20°S and 80°N in different experiments. (a) CTRL, (b) 60N, (c) 60NS, (d) GLOB. The grey bold line denotes the position where the meridional overturning stream function transport is zero.

3.2 Stratification adjustment over Deep Convection regions

Anthropogenic greenhouse effect modifies the temperature and salinity fields (Li et al., 2020), and the weakening of AMOC can be better understood by exploring the adjustment of deep convections to to temperature and salinity variations (Haskins et al., 2020). The vertical stratification changes can provide insights into the weakened deep convection. Consequently, we calculate the squared buoyancy frequency (N^2) (Equation 1) of the water column associated with the deep convection intensity (Levang & Schmitt, 2020), and assess the relative contribution of temperature and salinity in the evolution of stratification (Equations 2 and 3). The results show that 4×CO2 forcing has indeed led to a strong enhancement of the ocean stratification in Nordic

Seas and Labrador Sea deep convective zones, showing positive buoyancy anomalies (Figures 2a and 2d). A thin layer of strong N^2 increase appears at 200-1000 m with a maximum value of around 300 m, indicating a notable increase of the upper ocean stratification. The convection activities can be greatly suppressed since the stratified layer acts as an effective barrier, limiting the downwelling of surface water that sinks to the deep layer.

In 60N, the deep convection is still maintained as the upper ocean stratification exhibits small variations when 4×forcing is applied in Arctic (Figures 2a and 2b). Changes in outflow induced by Arctic warming, such as the cold fresh East Greenland Current originating from the Arctic (Schlichtholz & Houssais, 1999), may have almost negligible effects on the mixing in deep convection zones. When warming forcing is applied outside the Arctic, warming and salinization in 60NS is far stronger than in 60N. The anomalously strong stratification of the subsurface and intermediate layers rather than the surface layer in 60NS and GLOB run reflects the advective response of AMOC to the warm and salty water carried by the North Atlantic current in the upper limb. The stratification enhancement is particularly remarkable in 60NS and GLOB runs, and the vertical stratification in 60N is generally consistent with CTRL, suggesting that the anomalous changes in the deep convection zones are mostly dominated by extra-Arctic warming.

Comparing two areas in all the experiments, it is clear that the interplay of temperature changes which lead to a lower density, and salinity changes which densify the upper layer, sets the magnitude of AMOC weakening. The convective mixing at Nordic Seas is entirely thermally driven since the salinity effect always plays an opposite role in the upper ocean ($\overline{N_t^2} > 0, \overline{N_s^2} < 0$) (Figures 2a-c). In 60N, the temperature and salinity changes are almost negligible, and the vertical gradient is largely identical to that of CTRL. Temperature anomalies of 6-7°C and

salinity anomalies of 0.3-0.4 psu appear in 60NS and GLOB experiments (subplots inserted in Figures 2b and 2c). The temperature-induced stratification ($\overline{N_t^2}$) in 60NS and GLOB could be even twice the total $\overline{N^2}$, some of which (~45%) is offset by the salinity-induced stratification (N_s^2). The warming effect is mainly in the upper ocean, with relatively slight changes in deep ocean.

Whereas, a more complex vertical stratification emerges at Labrador Sea deep convection zone, with a structure like a double maximum of $\overline{N^2}$ (Figure 2d). The upper ocean stratification is reinforced by the temperature and salinity jointly. warming and salinization extend from surface to around 2500 m (subplots inserted in Figures 2e and 2f), which lead to strong temperature and salinity stratification ($\overline{N_t^2} > 0, \overline{N_s^2} > 0$) both in the upper 1500 m and in the deep layer within 1500-2500 m (Figures 2e and 2f). The deep layer changes which may related to the deep branch of AMOC (Levang & Schmitt, 2020). Due to enhanced intrusion of Antarctic Bottom Water (AABW) (Haskins et al., 2020), the cold and fresh anomalies result in an unstable vertical salinity gradient ($\overline{N_t^2} > 0, \overline{N_s^2} < 0$). However, the temperature contribution overcompensates the salinity component to reach a state of intensified deep ocean stability (Figures 2d-2f). Deep convection activities in Nordic Seas appear to be more sensitive to the greenhouse gas forcing than that in the Labrador Sea (Figures 2a and 2d). In idealized sensitivity experiments, especially in 60NS and GLOB, deep convective depth in the Nordic Seas drops to around 500 m dramatically, while in the Labrador Sea it can still be maintained at around 1000 m. Therefore, the weakening of AMOC may mainly result from the reduced deep-water formation over Nordic Seas in warming climate. Lique & Thomas (2018) have also predicted that the deep convection in Nordic Sea may disappear or even undergo a latitudinal shift in warming forcing scenarios.

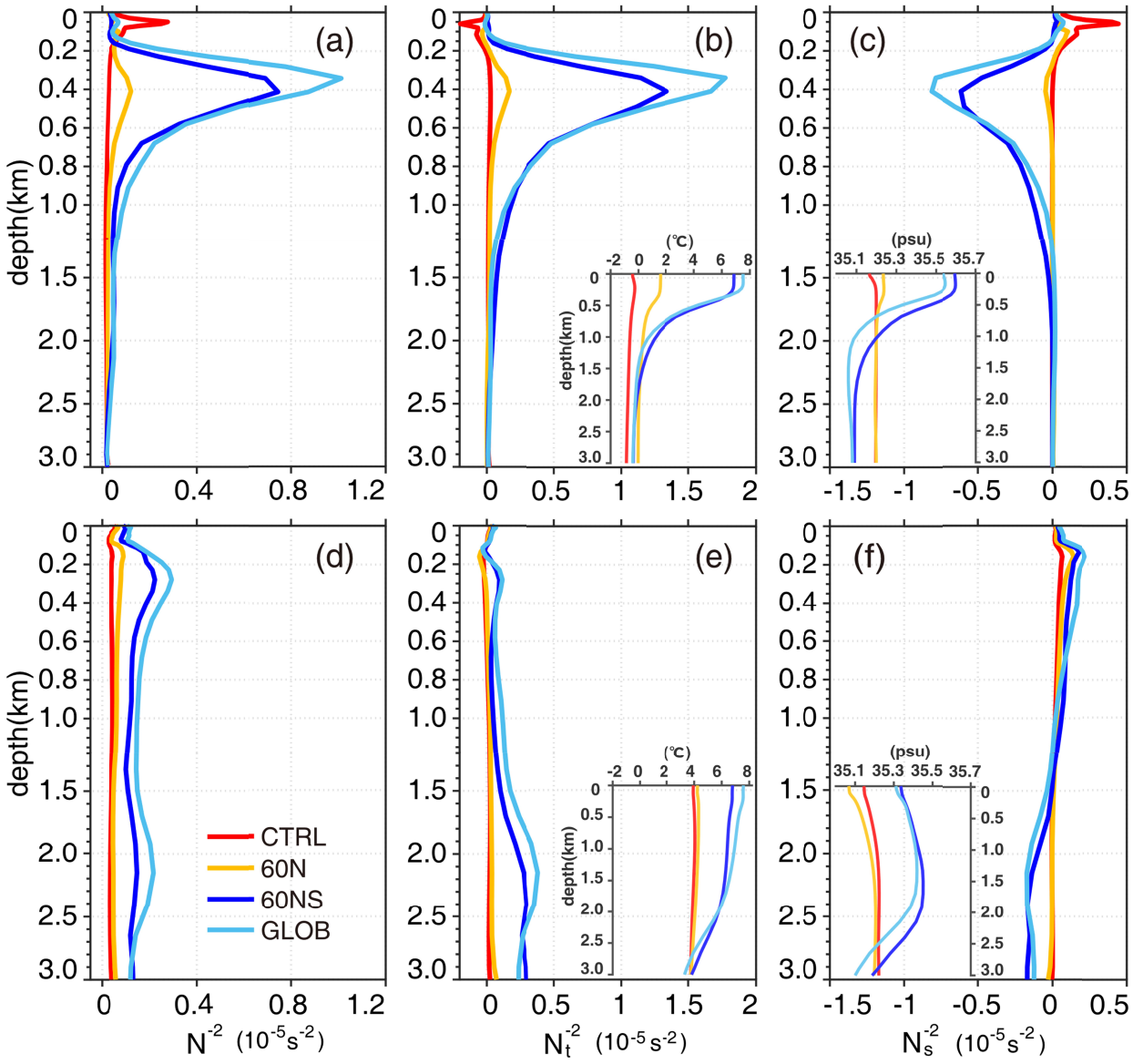

Figure 2. Climatology wintertime stratification at deep convection zones. (a) regionally weighted average squared buoyancy frequency ($\overline{N^2}$, $10^{-5}s^{-2}$) throughout all depth at Nordic Seas, (b) the temperature component of $\overline{N^2}$, defined as $\overline{N_t^2}$, (c) the salinity component of $\overline{N^2}$,defined as $\overline{N_s^2}$. The subplots inserted in (b) and (c) are the corresponding profiles of potential temperature and salinity. (d), (e) and (f) same as (a), (b), and (c), but for the Labrador Sea deep convection zone. Note the different ranges of x-axis in the three columns.

3.3 Heat Budget of the Upper-Ocean

The increase of ocean heat content (OHC) in the upper Nordic Seas and Labrador Sea is widespread (Supplementary Figure S2). To assess the impact of different thermodynamic and dynamic processes on deep convection, we analyze the source of OHC variability in subpolar region (Supplementary Text S2). Heat budget analysis reveals that the low-frequency variability of OHC is mainly influenced by the integrated effect of anomalous horizontal thermal advection transport (HT) and local air-sea heat fluxes (HF) (Supplementary Figure S3) (Desbruyères et al., 2015; Foukal & Lozier, 2018; Marsh et al., 2008). Two closed areas are therefore selected in the upper 700 m (i.e., the upper limb of overturning circulation) of the Nordic Seas and Labrador Sea, respectively (Figure 3, shaded area in the inserted map). Our main concern is how the Arctic and extra-Arctic warming influence these two main factors and the convection activities, which in turn modulates the AMOC weakening. Note that positive values of HT and HF are defined as the heat input to the ocean box through the cross-sections and air-sea interface. In other words, the negative value of HF means that the ocean loses heat to the atmosphere.

In Nordic Seas, the local variability in CTRL run is mainly controlled by the net surface HF, which is even twice as high as HT (HT=104 TW, HF=−245 TW). In 60N, both the slight increase in advective HT and the decrease in HF are no more than 10 TW, the changes mostly offsetting each other. Arctic warming effects are mainly confined to local areas, with relatively limited impacts on AMOC. However, when 4×CO2 forcing applied in extra-Arctic (60NS), the relative contribution of the two factors changes a lot compared to CTRL. As the ocean warms (subplots inserted in Figures 3b), the temperature difference at the air-sea interface decreases leading to a weaker heat exchange. Opposite variation of latent and sensible heat fluxes and almost negligible variations in long wave and short wave radiation makes the HF at Nordic Seas

insensitive to the regional forcings. The local HF change is much smaller and less than 10% than that of HT, the net air-sea HF in Nordic Seas is thus not predominant in dampening the convective mixing in global warming. On the other hand, the advection transports a substantial amount of heat to the closed region through the southern transect (N2), increasing by more than a factor of two compared to the CTRL simulation. Increased advective heat input and reduced heat loss from the ocean to atmosphere lead to a considerable OHC increase and large amounts of heat trapped in the Nordic Seas (Figure 3a). And the changes in 60NS are similar to those in GLOB, when warming forcing involving extra-Arctic regions, the upper limb of AMOC (i.e., North Atlantic Current (NAC)) (Chafik et al., 2014) carries warm and salty water northward into the Arctic. Although the AMOC decline acts to decrease the northward volume transport into the subpolar region (Supplementary Figure S4), it is apparent that the heat transport by the weakening AMOC becomes more efficient as its upper branch warms. A large amount of heat transport is achieved by the positive temperature flux through the southern flank at Denmark Strait and Iceland-Faroe Ridge. More heat and salt are trapped in the Nordic Seas in terms of circulation transport, contributing to the warming and salinization of the upper ocean (Figures 2b and 2c) and further reinforcing stabilization of the stratification.

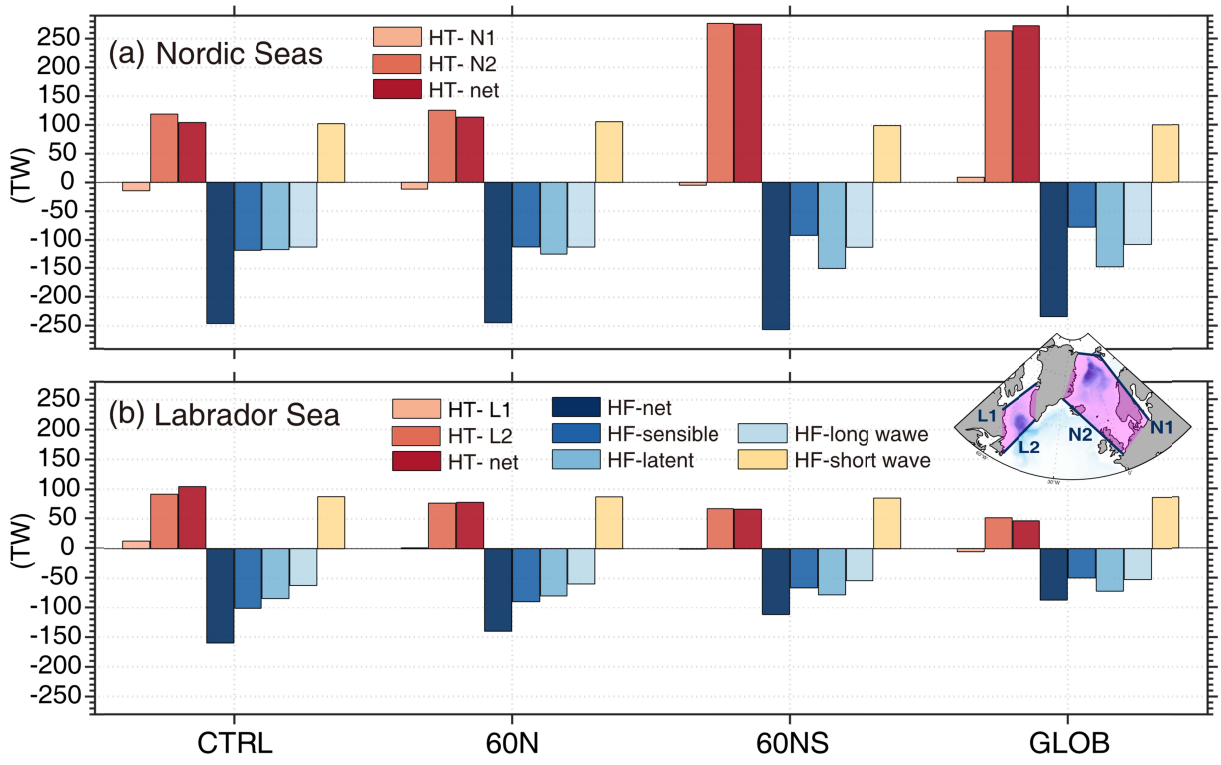

Figure 3. Two main components of the upper ocean heat budget at the irregularly closed region in different experiments (29°-5°W, 56°-80°N at Nordic Seas, 64°-43°W, 53°-67°N at Labrador Sea, upper 700 m). (a) advection heat transport (HT) and ocean surface heat flux (HF) into the closed region of Nordic Seas (positive, inward, heat gain of the region). The HT-N1, HT-N2, and HT-net represent the heat transport across the N1, N2 sections, and the sum of these two sections. The HT-net, HT-sensible, HT-latent, HT-long wave, and HT-short wave represent the net ocean surface heat flux and the components that account for it (the sensible, latent heat flux and the long wave and short wave radiation flux). (b) The same as (a), but for the closed region of Labrador Sea included in the sections marked as L1 and L2. The closed areas of the Nordic Seas and Labrador Sea are shown as shaded on the inserted map.

The Labrador Sea features a different regime of adjustment. In CTRL run, the influence of HF is relatively stronger than the HT (HT=104, HF=−160 TW). As in the case of Nordic Seas, the

impact of Arctic warming (60N) on deep convection in Labrador Sea is quite small compared to extra-Arctic warming (60NS). In GLOB, the local HF response is noticeable (halved compared to CTRL), and the magnitude of the percentage response is comparable to the HT, but in absolute terms even exceeds the HT response by about 20 TW. In all the sensitivity experiments, both advective HT and oceanic HF are decreased, i.e., less advective heat gain of the closed region is accompanied by less oceanic heat loss to the atmosphere, which may partially compensate each other (Figures 3b). Even though the weakening of advection heat transport facilitates deep convection, the reduction of the air-sea heat flux in winter increases ocean heat gain and contributes to enhanced stratification. The stronger stratification in the upper Labrador Sea suggests that it is the HF changes that play a more important role. By the time NAC enters subpolar region, the mainstream heads northeastward enhanced. The rest feeds the cyclonic circulation in the Iceland Basin and the flow over Reykjanes Ridge into the Irminger Sea (Daniault et al., 2016). The branches that form in the Irminger Sea and Iceland Basin along the Greenland boundary (Chafik & Rossby, 2019) towards the Labrador Sea (L2 section) weakened (Supplementary Figure S4). Owing to the relatively long distance from the east to the west subpolar region and the ocean heat loss along the way (Supplementary Figure S3), the accumulation of advection heat transport that intrude into the Labrador Sea decreases and does not result in great changes in water properties (Figures 2b, c and 2e, f). It also helps to understand the OHC anomalies of the upper ocean, with the Labrador Sea showing a weaker thermal content increase than in the Nordic Seas (Supplementary Figure S2).

4 Conclusions

Based on the idealized sensitivity experiments, we quantify the transient AMOC response to the sudden increase of regional 4×CO2 forcings in the initial century. The AMOC intensity

displays different degrees of decline under regional warming forcings. Thermohaline variations over deep convection zones lead to stronger stratification and enhanced stability of the upper ocean, which may effectively inhibit deep-water formation. We highlight that the NAC plays a key role in linking North Atlantic deep convection anomalies to changes in the AMOC strength on century timescales. According to the results of our sensitivity experiments, more than 65% of AMOC weakening can be attributed to the extra-Arctic warming. The effect of Arctic warming is more localized, and the impact of increased advection heat transport due to the extra-Arctic warming is overwhelming.

The increased stratification of upper ocean at Nordic Seas and Labrador Sea suggests that warming holds back the deep convection activities in the subpolar region. By heat budget analysis in closed regions of both deep convective zones, we reveal the dominant role of advection heat transport from the southern face of the North Atlantic for the weakening of vertical mixing or deep convection. However, the local variations in the two deep convection areas show different adjustment mechanisms in the warming scenario. In Nordic Seas, negligible changes in sea-air fluxes occur, while substantial increases by a factor of two in advective heat transport from the southern side into the Nordic Seas are simulated that dominate upper ocean heat content changes. Accordingly, the temperature stratification variability induced by extra-Arctic warming can largely be responsible for the local buoyancy increases and convection weakening. In Labrador Sea, the decrease in advective heat transport into the region and the heat gain from less heat loss to the atmosphere can partially balance each other. The local heat flux changes are predominant in this region, as deep convection remains suppressed, but not as strongly as in Nordic Seas. In the idealized global warming scenario, more heat is transported into Nordic Seas by the northward branch of NAC and dominates the local changes. Another major branch of NAC that enters the

Labrador Sea along East Greenland topography (Chafik et al., 2014; Curry & Mauritzen, 2005) weakens, and less heat enters the region in the form of advection transport after a somewhat oceanic heat loss along the way. The effects of net surface heat fluxes and advective heat transport variations on upper ocean stratification compensate each other to a large extent. This further explains the much stronger stratification in Nordic Seas than in Labrador Sea under warming conditions. Overall, different mechanisms of deep convection weakening in these two ocean areas eventually contribute to the weakening of AMOC, which is primarily cause by the reduced deep convection activities in Nordic Seas in a global warming scenario. Note that the freshwater input from Greenland is not considered in the simulations, which may affect local stratification somewhat.

From the perspective of the evolution of deep convective activity in the subpolar North Atlantic, we investigate the possible response mechanism of AMOC in global warming scenarios, which may serve as a reference for climate projection. AMOC is a large-scale ocean circulation that shows response times on a century and even millennium scale (Bonan et al., 2022; He et al., 2019; Lique & Thomas, 2018). Here, we discuss the response of AMOC to climate warming on centennial scale, a time scale over which most of the GCMs show a decline of AMOC as response to abrupt 4xCO2 forcing before they diverge to either recovered or further diminished AMOC states (Bonan et al., 2022). More generally, the response of the ocean to the warming forcing results from a complex combination of various mechanisms such as tropical precipitations, local overflow, as well as subpolar circulation changes (Daniault et al., 2016; Levang & Schmitt, 2020; Yeager et al., 2021). The relative contribution of the deep convective zones to the transformation of the deep-water in North Atlantic is also a matter that remains to be clarified. Further detailed assessment of high-resolution models and observational supports are

needed (Lozier et al., 2019; Sallée et al., 2021). Interestingly, the 4×CO2 in sensitivity experiments is held constant for the simulation, but the weakening of the AMOC is not sustained, instead, recovery occurs. This implies that there is still a certain mechanism or other sources of convection and deep-water formation to maintain AMOC (Bonan et al., 2022), which is probably not driven by subpolar North Atlantic dynamics because the convection deepens at other latitudinal belts (Lique & Thomas, 2018). Our simulation results also show regions of enhanced convection in the Arctic and subtropical regions (not shown), probably another topic worth further exploring. It will be beneficial to explore regions of enhanced convection in the Arctic and subtropical regions that occur in our simulation results in a subsequent study.

Acknowledgments

The study is supported by National Key R&D Program of China (2022YFE0106400), the Opening Project of Key Laboratory of Marine Science and Numerical Modeling, MNR (2020-ZD-01) and the National Natural Science Foundation (41776004). We are grateful to the DKRZ (German computing center) for providing us with computing time. This work has been carried out within the EU project APPLICATE.

Open Research

The climate model simulation data used in this study could be downloaded from the website https://doi.org/10.5281/zenodo.7657530.

References

Bonan, D. B., Thompson, A. F., Newsom, E. R., Sun, S., & Rugenstein, M. (2022). Transient and equilibrium responses of the Atlantic overturning circulation to warming in coupled

363 climate models. *Journal of Climate*, *35*(15), 5173–5193.
364 https://doi.org/10.1175/JCLI-D-21-0912.1
365 Caesar, L., & Rossby, T. (2019). Volume, heat, and freshwater divergences in the subpolar North
366 Atlantic suggest the Nordic Seas as key to the state of the meridional overturning
367 circulation. *Geophysical Research Letters*, *46*(9), 4799–4808.
368 https://doi.org/10.1029/2019GL082110
369 Chafik, L., Rossby, T., & Schrum, C. (2014). On the spatial structure and temporal variability of
370 poleward transport between Scotland and Greenland. *Journal of Geophysical Research:*
371 *Oceans*, *119*(2), 824–841. https://doi.org/10.1002/2013JC009287
372 Chen, X., & Tung, K. (2018). Global surface warming enhanced by weak Atlantic overturning
373 circulation. *Nature*, *559*(7714), 387–391. https://doi.org/10.1038/s41586-018-0320-y
374 Curry, R., & Mauritzen, C. (2005). Dilution of the northern North Atlantic ocean in recent
375 decades. *Science*, *308*(5729), 1772–1774. https://doi.org/10.1126/science.1109477
376 Daniault, N., Mercier, H., Lherminier, P., Sarafanov, A., Falina, A., Zunino, P., et al. (2016). The
377 northern North Atlantic Ocean mean circulation in the early 21st century. *Progress in*
378 *Oceanography*, *146*, 142–158. https://doi.org/10.1016/j.pocean.2016.06.007
379 Desbruyères, D., Mercier, H., & Thierry, V. (2015). On the mechanisms behind decadal heat
380 content changes in the eastern subpolar gyre. *Progress in Oceanography*, *132*, 262–272.
381 https://doi.org/10.1016/j.pocean.2014.02.005
382 Durack, P. J. (2015). Ocean salinity and the global water cycle. *Oceanography*, *1*(28), 20–31.
383 Fofonoff, N., & Millard, R. (1983). Algorithms for computation of fundamental properties of
384 seawater. *Unesco Technical Papers in Marine Sciences*, *44*.

385 Foukal, N. P., & Lozier, M. S. (2018). Examining the origins of ocean heat content variability in
386 the eastern North Atlantic subpolar gyre. *Geophysical Research Letters*, *45*(20).
387 https://doi.org/10.1029/2018GL079122
388 Haskins, R. K., Oliver, K. I. C., Jackson, L. C., Wood, R. A., & Drijfhout, S. S. (2020).
389 Temperature domination of AMOC weakening due to freshwater hosing in two GCMs.
390 *Climate Dynamics*, *54*(1–2), 273–286. https://doi.org/10.1007/s00382-019-04998-5
391 He, C., Liu, Z., & Hu, A. (2019). The transient response of atmospheric and oceanic heat
392 transports to anthropogenic warming. *Nature Climate Change*, *9*(3), 222–226.
393 https://doi.org/10.1038/s41558-018-0387-3
394 Jansen, M. F., Nadeau, L., & Merlis, T. M. (2018). Transient versus equilibrium response of the
395 ocean's overturning circulation to warming. *Journal of Climate*, *31*(13), 5147–5163.
396 https://doi.org/10.1175/JCLI-D-17-0797.1
397 Levang, S. J., & Schmitt, R. W. (2020). What causes the AMOC to weaken in CMIP5? *Journal*
398 *of Climate*, *33*(4), 1535–1545. https://doi.org/10.1175/JCLI-D-19-0547.1
399 Li, G., Cheng, L., Zhu, J., Trenberth, K. E., Mann, M. E., & Abraham, J. P. (2020). Increasing
400 ocean stratification over the past half-century. *Nature Climate Change*, *10*(12), 1116–
401 1123. https://doi.org/10.1038/s41558-020-00918-2
402 Lique, C., & Thomas, M. D. (2018). Latitudinal shift of the Atlantic Meridional Overturning
403 Circulation source regions under a warming climate. *Nature Climate Change*, *8*(11),
404 1013–1020. https://doi.org/10.1038/s41558-018-0316-5
405 Liu, W., Fedorov, A. V., Xie, S.-P., & Hu, S. (2020). Climate impacts of a weakened Atlantic
406 Meridional Overturning Circulation in a warming climate. *Science Advances*, *6*(26),
407 eaaz4876. https://doi.org/10.1126/sciadv.aaz4876

Lozier, M. S., Li, F., Bacon, S., Bahr, F., Bower, A. S., Cunningham, S. A., et al. (2019). A sea change in our view of overturning in the subpolar North Atlantic. *Science*, *363*(6426), 516–521. https://doi.org/10.1126/science.aau6592

Marsh, R., Josey, S. A., de Cuevas, B. A., Redbourn, L. J., & Quartly, G. D. (2008). Mechanisms for recent warming of the North Atlantic: Insights gained with an eddy-permitting model. *Journal of Geophysical Research*, *113*(C4), C04031. https://doi.org/10.1029/2007JC004096

McDougall, T. J. (1987). Neutral surfaces. *Journal of Physical Oceanography*, *17*(11), 1950–1964. https://doi.org/10.1175/1520-0485(1987)017<1950:NS>2.0.CO;2

McManus, J. F., Francois, R., Gherardi, J. M., Keigwin, L. D., & Brown Leger, S. (2004). Collapse and rapid resumption of Atlantic meridional circulation linked to deglacial climate changes. *Nature*, *428*(6985), 834–837. https://doi.org/10.1038/nature02494

Medhaug, I., Langehaug, H. R., Eldevik, T., Furevik, T., & Bentsen, M. (2012). Mechanisms for decadal scale variability in a simulated Atlantic meridional overturning circulation. *Climate Dynamics*, *39*(1), 77–93. https://doi.org/10.1007/s00382-011-1124-z

Petit, T., Lozier, M. S., Josey, S. A., & Cunningham, S. A. (2020). Atlantic deep water formation occurs primarily in the Iceland Basin and Irminger Sea by local buoyancy forcing. *Geophysical Research Letters*, *47*(22). https://doi.org/10.1029/2020GL091028

Rackow, T., Sein, D. V., Semmler, T., Danilov, S., Koldunov, N. V., Sidorenko, D., et al. (2019). Sensitivity of deep ocean biases to horizontal resolution in prototype CMIP6 simulations with AWI-CM1.0. *Geoscientific Model Development*, *12*(7), 2635–2656. https://doi.org/10.5194/gmd-12-2635-2019

Sallée, J.-B., Pellichero, V., Akhoudas, C., Pauthenet, E., Vignes, L., Schmidtko, S., et al. (2021). Summertime increases in upper-ocean stratification and mixed-layer depth. *Nature*, *591*(7851), 592–598. https://doi.org/10.1038/s41586-021-03303-x

Schlichtholz, P., & Houssais, M. (1999). An investigation of the dynamics of the East Greenland Current in Fram Strait based on a simple analytical model. *Journal of Physical Oceanography*, *29*(9), 2240–2265. https://doi.org/10.1175/1520-0485(1999)029<2240:AIOTDO>2.0.CO;2

Semmler, T., Pithan, F., & Jung, T. (2020). Quantifying two-way influences between the Arctic and mid-latitudes through regionally increased CO2 concentrations in coupled climate simulations. *Climate Dynamics*, *54*(7–8), 3307–3321. https://doi.org/10.1007/s00382-020-05171-z

Semmler, T., Danilov, S., Gierz, P., Goessling, H. F., Hegewald, J., Hinrichs, C., et al. (2020). Simulations for CMIP6 with the AWI climate model AWI-CM-1-1. *Journal of Advances in Modeling Earth Systems*, *12*(9). https://doi.org/10.1029/2019MS002009

Semmler, T., Jungclaus, J., Danek, C., Goessling, H. F., Koldunov, N. V., Rackow, T., & Sidorenko, D. (2021). Ocean model formulation influences transient climate response. *Journal of Geophysical Research: Oceans*, *126*(12). https://doi.org/10.1029/2021JC017633

Smedsrud, L. H., Muilwijk, M., Brakstad, A., Madonna, E., Lauvset, S. K., Spensberger, C., et al. (2022). Nordic Seas heat loss, Atlantic inflow, and Arctic sea ice cover over the last century. *Reviews of Geophysics*, *60*(1). https://doi.org/10.1029/2020RG000725

Solomon, S., Plattner, G. K., Knutti, R., & Friedlingstein, P. (2009). Irreversible climate change due to carbon dioxide emissions. *Proceedings of the National Academy of Sciences*, *106*(6), 1704–1709. https://doi.org/10.1073/pnas.0812721106

Stuecker, M. F., Bitz, C. M., Armour, K. C., Proistosescu, C., Kang, S. M., Xie, S.-P., et al. (2018). Polar amplification dominated by local forcing and feedbacks. *Nature Climate Change*, *8*(12), 1076–1081. https://doi.org/10.1038/s41558-018-0339-y

Suzuki, T., Komuro, Y., Kusahara, K., & Tatebe, H. (2022). Transient influence of the reduction of deepwater formation on ocean heat uptake and heat budgets in the global climate system. *Geophysical Research Letters*, *49*(3). https://doi.org/10.1029/2021GL095179

Thomas, L., & Ferrari, R. (2008). Friction, frontogenesis, and the stratification of the surface mixed layer. *Journal of Physical Oceanography*, *38*(11), 2501–2518. https://doi.org/10.1175/2008JPO3797.1

Thomas, M., Tregiuer, A., Blanke, B., Deshayes, J., & Voldoire, A. (2015). A lagrangian method to isolate the impacts of mixed layer subduction on the meridional overturning circulation in a numerical model. *Journal of Climate*, *19*(28), 7503–7517. https://doi.org/10.1175/JCLI-D-14-00631.1

Thomas, M. D., & Fedorov, A. V. (2019). Mechanisms and impacts of a oartial AMOC recovery under enhanced freshwater forcing. *Geophysical Research Letters*, *46*(6), 3308–3316. https://doi.org/10.1029/2018GL080442

Wang, Q., Danilov, S., Sidorenko, D., Timmermann, R., Wekerle, C., Wang, X., et al. (2014). The Finite Element Sea Ice-Ocean Model (FESOM) v.1.4: formulation of an ocean general circulation model. *Geoscientific Model Development*, *7*(2), 663–693. https://doi.org/10.5194/gmd-7-663-2014

Wang, X., Wang, Q., Sidorenko, D., Danilov, S., Schröter, J., & Jung, T. (2012). Long-term ocean simulations in FESOM: evaluation and application in studying the impact of Greenland Ice Sheet melting. *Ocean Dynamics*, *62*(10–12), 1471–1486. https://doi.org/10.1007/s10236-012-0572-2

Yashayaev, I. (2007). Hydrographic changes in the Labrador Sea, 1960–2005. *Progress in Oceanography*, *73*(3–4), 242–276. https://doi.org/10.1016/j.pocean.2007.04.015

Yashayaev, I., & Loder, J. W. (2017). Further intensification of deep convection in the Labrador Sea in 2016. *Geophysical Research Letters*, *44*(3), 1429–1438. https://doi.org/10.1002/2016GL071668

Yeager, S., Castruccio, F., Chang, P. P., Danabasoglu, G., Maroon, E., Small, J., et al. (2021). An outsized role for the Labrador Sea in the multidecadal variability of the Atlantic overturning circulation. *Science Advances*, *7*. https://doi.org/10.1126/sciadv.abh3592

Zhao, J., Bower, A., Yang, J., Lin, X., & Penny Holliday, N. (2018). Meridional heat transport variability induced by mesoscale processes in the subpolar North Atlantic. *Nature Communications*, *9*(1), 1124. https://doi.org/10.1038/s41467-018-03134-x